P–V–T Behavior of Secondary Transitions in Amorphous Polymers. 3. Temperature Dependence of the Tait Parameter, b, at $T > T_g$

Raymond F. Boyer

Michigan Molecular Institute, Midland, Michigan 48640. *Received October 7, 1980; Revised Manuscript Received October 5, 1981*

ABSTRACT: Values of the Tait parameter, b, in bars, calculated from a linear form of the Tait equation at $P \leq 400$ bars (hence as $P \rightarrow 0$) are found to decrease with increasing temperature along a two straight line path intersecting at the liquid–liquid transition temperature, T_{ll}. Since b is about one-tenth the bulk modulus, $\bar{K}$, this means that the temperature variation of $\bar{K}$ is less above T_{ll} than below it. Conversely, the isothermal compressibility increases more rapidly above T_{ll} than below it. b–T behavior for a series of polymers is most conveniently compared by using a reduced temperature scale, T (K)/T_{ll} (K). The magnitude of b in bars at T_{ll} increases approximately as the cube of the polymer density at T_{ll}. The change in slope, $\Delta(db/dT)$, across T_{ll} is a general measure of the strength of T_{ll}, being least for PS's and PVAc and greatest for the polymethacrylate esters. It is shown that the conventional linear ln b–T representation is a good approximation to the two straight lines, mainly because of the small range in b values for any given polymer. However, the two lines intersecting at T_{ll} are mathematically correct and indicate that the slopes of the bulk modulus, $\bar{K}$, and the isothermal compressibility, κ, as a function of temperature change at T_{ll}. The temperature dependence of b at $P \rightarrow 0$ provides convenient thermodynamic-type evidence for T_{ll} on polymers for which tabulated P–V–T data are available.

Introduction

This paper is concerned with the temperature dependence of the Tait equation parameter, b, calculated from volume–pressure isotherms in the liquid or $T > T_g$ state of amorphous polymers. Contrary to earlier findings in the literature which treat b as decreasing exponentially with temperature, we demonstrate that it decreases along two straight lines which intersect at the liquid–liquid transition temperature, T_{ll}. b is calculated herein at moderate pressures, $P \leq 400$ bars, to obtain a value of b as $P \rightarrow 0$, i.e., before any pressure-induced transition can seriously alter the value of b.

The Tait equation has been widely used to represent isothermal volume–pressure data on polymers.[1-14] Following Simha and collaborators,[5-10] we write the Tait equation for isothermal conditions as

$$1 - V/V_0 = C' \ln (1 + P/b); \quad T = \text{constant} \qquad (1)$$

where V is the specific volume in cm^3 g^{-1} at pressure P (in bars), V_0 is the corresponding quantity at a reference pressure, usually $P = 1$ bar, C' is a constant with a universal value of 0.0894, and b is the parameter under discussion. b is considered to be constant across any isotherm for which there is no pressure-induced transition.

Wood[2] derived from eq 1 the relationship

$$\bar{K} = b/C' + P/C' \qquad (2)$$

where $\bar{K}$ is the bulk modulus, defined as $[-(1/V_0)(\partial V/\partial P)]^{-1}$. Thus b is proportional to $\bar{K}$ as $P \rightarrow 0$. All subsequent discussion about variation of b with T at $P \rightarrow 0$ acquires enhanced physical meaning if considered as equivalent to the temperature dependence of $\bar{K}$.

b decreases with temperature from values of 3000–4000 bars below T_g to as low as 800–1000 bars well above T_g. Typical behavior for PS, PMMA, and PVC has been summarized by Simha et al.[7] As first proposed by Gee[4] and subsequently employed by Simha et al.[5-10] and then by Beret et al.,[11,12] the liquid-state variation of b is commonly expressed as

$$b = A \exp(-\gamma T) \qquad (3)$$

where A and γ are constants. Table I collects these constants for the polymers to be discussed herein and cites specific literature references.

Table I
Literature Values of Liquid-State A and γ Parameters for Eq 3[a]

polymer[b]	ref	A_1,[c,d] bars	$-\gamma$,[c,d] K^{-1}	$-A\gamma$[e]
1. PnBMA	10	2267	5.34×10^{-3}	12.115
2. PVAc	8	2035	4.257×10^{-3}	8.663
3. PVAc	11	2231	3.4315×10^{-3}	7.656
4. iso-PMMA	9	2992	4.56×10^{-3}	13.64
5. a-PS	6	2169	3.319×10^{-3}	7.199
6. a-PS	7	2435	4.14×10^{-3}	10.09
7. a-PMMA	10	2875	4.146×10^{-3}	11.920
8. PCHMA	10	2952	5.220×10^{-3}	15.409
9. PoMS	6	2619	4.11×10^{-3}	10.77

[a] Glassy-state values of A and γ appear in the same references. [b] Arranged in order of increasing T_g. [c] Calculated by using average values of b for each isotherm, with C' from eq 1 having a value of 0.0894 except for item 3, ref 11, where C is 0.104623. [d] Values of A and γ using b^* values calculated from eq 4 at $P \leq 400$ bars appear in Table IV. [e] The slope of eq 3 is $db/dT = -A\gamma \exp(-\gamma T)$.

Quach and Simha[5,6] were the first, to our knowledge, to indicate the presence of a secondary transition in the liquid state which they called a low-pressure glass, T_g(LP), and the extrapolated existence of the β process above T_g at sufficiently high pressures for both PS and poly(*o*-methylstyrene). We subsequently[15,16] generalized these findings to other polymers and added evidence for the existence of the liquid–liquid or T_{ll} transition (see Figure 2 of ref 15). We suggested that b (hence $\bar{K}$) increased moderately at these secondary transitions just as Quach and Simha had shown for T_β below T_g.[5,6] This implied that the Tait equation did not hold exactly for the liquid state even though it was an extremely good approximation to most V–P data.

Previous papers in this series[15,16] employed variations of and approximations to eq 1 for the purpose of locating intersection pressures, P_i, along V–P isotherms corresponding to pressure-induced transitions. Major emphasis was on the liquid–liquid transition and its pressure coefficient, dT_{ll}/dP. Background material on T_{ll} appears in ref 17–27, with ref 17, 19, and 22 being reviews.

0024-9297/82/2215-0774$01.25/0

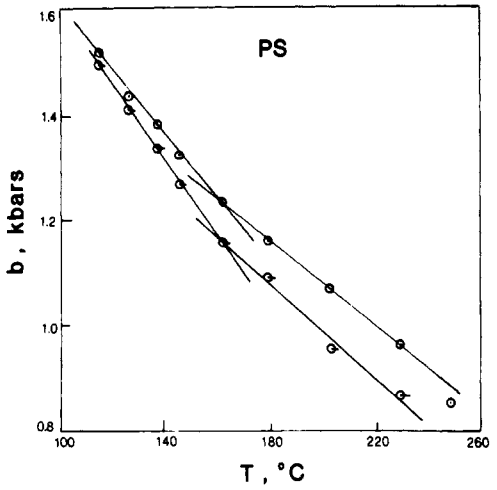

Figure 1. Top, Tait parameter, b, as a function of T for atactic polystyrene, using b values reported by Simha et al.[7] at $T > T_g$; bottom, b^* at $P \leq 400$ bars calculated from the same P–V–T data by eq 4.

Since b is not always constant across any isotherm which we have thus far examined, attention is focused herein on initial values of b calculated somewhat arbitrarily for $P \leq 400$ bars as generally representative of b at $P \rightarrow 0$. Such b values are calculated from a linear form of the Tait equation

$$Y = \exp[1/C'(1 - V/V_0)] - 1 = P/b \qquad (4)$$

proposed to us by Šolc.[28] Parenthetically, we have employed eq 4 to reexamine all V–P isotherms previously considered by other methods[15,16] with the same conclusion as before, namely, that many liquid-state isotherms of polymers do not follow the Tait equation. This fact is manifested by one or more sharp slope changes in eq 4 type plots.

The present inquiry began with casual linear plotting of b vs. T at $T > T_g$ for polystyrene (PS), using tabulated values of b given by Simha et al.[7] This plot appeared to us to consist of two straight-line sections intersecting at or near the T_{II} value for PS. No details were given by the authors[7] as to how b was calculated but we assumed that b was an average value considered representative of each isotherm. Figure 1 plots their values of b calculated from the experimental data of Hellwege et al.[14] as a function of T (upper plot) as well as our values of b at $P \leq 400$ bars calculated from the same data via eq 4. The Simha et al. values[7] are consistently higher than ours, presumably because they have been increased by one or more pressure-induced transitions.

Regression analysis for the two upper lines gave slopes of −6.340 and −4.305 bars K^{-1}, correlation coefficients, R^2, of 0.99321 and 0.99668, and standard errors for b of 8.310 and 10.172 bars, that is, about 1%. At the same time, Simha et al.[7] showed that the same b–T values could be represented by eq 3 with parameters listed in Table I. The maximum difference between b determined from the P–V–T data and b calculated by an eq 3 treatment was 17 bars, with the average being 9.9 bars. These differences became systematically larger with increasing temperature. However, linear regression of the ln b–T values of Simha et al. gave $R^2 = 0.99631$ and a standard error of 0.12608 bar. Thus the two-line method and the ln b–T method gave roughly equivalent results. Subsequently, as detailed herein, b–T data on other polymer systems were analyzed by the same two procedures, with similar conclusions. This seeming dichotomy between the two-line representation of b vs. T and the one-line representation of ln b vs. T was of considerable concern to us. A resolution of this paradox is offered in Appendix I, but only after we had demonstrated the statistical validation of the two-line plots.

Details of Calculating b

Using all liquid-state isothermal V–P data starting 10–15 K above T_g at $P = 1$ bar, we calculated values of b by eq 4 for each available pressure from 1 to 400 bars inclusive. These several values of b were averaged after discarding any value markedly out of line. These average values of b for $P \leq 400$ bars are designated throughout as b^* to differentiate them from values of b calculated by other methods or computed by eq 4 at pressures above 400 bars. Plots of b^* vs. T show visual evidence for two-line behavior. Plots of ln b^* usually show visual evidence for a single line. However, all b^*–T and ln b^*–T data were subjected to computerized regression analysis in order to quantify the exactness of the fits. Linear, quadratic, and cubic fits were compared with two- and three-line fits for b^*–T and with linear fits for ln b^*–T in order to determine which resulted in smaller standard errors. In those cases for which there was a large enough number of liquid-state isotherms, point-to-point derivatives, $\Delta b/\Delta T$, were computed. In several cases when the number of data points above or below T_{II} was too few or when there was unusual scatter in the data, we first obtained a least-squares fit to ln b^* vs. T and then calculated b values for each isotherm. Justification for this procedure appears in Appendix I.

Slopes of the b^*–T lines below T_{II} are designated $(db^*/dT)_I$ and those above T_{II} as $(db^*/dT)_{II}$. The difference $\Delta(db/dT)$ across T_{II} is considered to be a characteristic parameter that provides a measure of the strength of T_{II}.

Numerical Values of T_{II} and T_{II}'

Values of T_{II} are considered known for each of the several polymers studied herein from one or more of the following sources: (1) analysis of V–P isotherms to obtain T_{II} at each of several pressures followed by extrapolation to $P = 1$ bar;[15,16] (2) analysis of isobaric V–T data at several low pressures, including $P = 1$ bar;[32] and (3) various types of physical measurements recently summarized elsewhere.[17,19,22] Publications covering specific techniques are as follows: torsional braid analysis, ref 17 and 20; DSC on fused films, pp 522–8 of ref 17; infrared spectroscopy, ref 21; ^{13}C NMR spectroscopy, ref 23; ESR spectroscopy, ref 24; zero-shear melt viscosity, ref 25; thermomechanical analysis, ref 26; and thermally stimulated current, ref 27.

Some of these papers also discuss a second liquid-state process, designated T_{II}' and lying some 50 K above T_{II}. See, for example, ref 17, 22, and 25. Evidence for T_{II}' in poly(n-butyl methacrylate) appears in Figure 3. We have proposed that T_{II} has an intermolecular origin, while T_{II}' is intramolecular.[22,25]

(4). Finally, as a consequence of studies in this paper, we can now recommend the intersection temperature of two-line b^*–T plots as a new technique for locating T_{II} on a thermodynamic basis from P–V–T data.

b–T Behavior for Specific Polymers

Polymers are discussed in the following order: (A) poly(cyclohexyl methacrylate) (PCHMA), (B) poly(n-butyl methacrylate) (PnBMA), (C) isotactic PMMA, (D) atactic thermal polystyrene (a-PS), (E) poly(o-methylstyrene) (PoMS), (F) poly(vinyl acetate) (PVAc), and (G) atactic PMMA. Various parameters for each set of data are assembled in Tables II–IV.

A. Poly(cyclohexyl methacrylate) (PCHMA). This polymer has isotherms over a relatively long glassy and

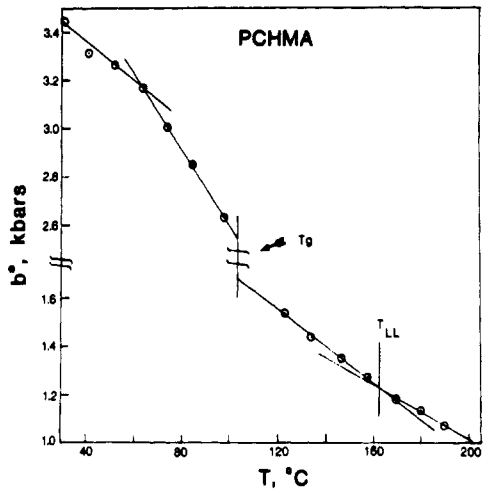

Figure 2. b^* for poly(cyclohexyl methacrylate) calculated from eq 4 for $P \leq 400$ bars, showing a discontinuity at T_g and slope changes both at a sub-T_g and at T_{ll}.

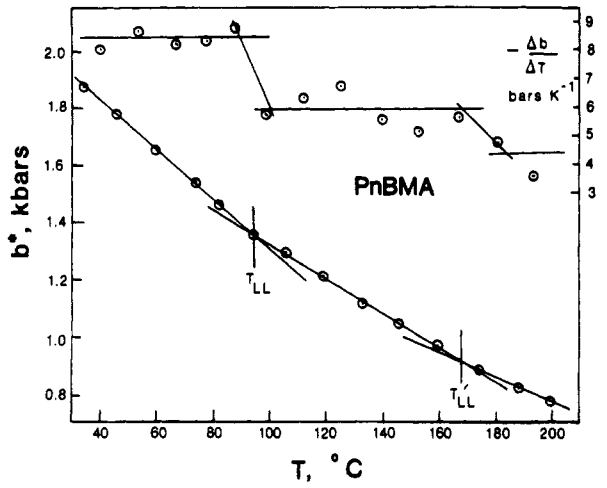

Figure 3. b^* vs. T for PnBMA from eq 4 for $P \leq 400$ bars, showing slope changes at the T_{ll} and T_{ll}' transition temperatures. Top curve shows the point-to-point derivatives, $\Delta b/\Delta T$, confirming the discontinuity at T_{ll} and possibly at T_{ll}'.

long liquid state. b^* vs. T is shown in Figure 2 to illustrate $T < T_g$, T_g, and $T > T_g$ behavior. The characteristic discontinuity in $\bar{K}$ at T_g is more commonly depicted in the literature[4] as a discontinuity in isothermal compressibility, $\kappa = -(1/V_0)(\partial V/\partial P)_T$. The slope change at $T_{ll} \sim 165$ °C is evident. The slope change at 62 °C was unexpected. However, Olabisi and Simha[10] reported a pressure-independent transition near 60 °C in PMMA. We therefore made plots of V_{sp}–T for several isobars of PCHMA starting at $P = 100$ bars. Distinct slope changes were observed near 60 °C. Hence, we suggest that a transition of unknown type exists near 60 °C at moderate pressures.

Figure 2 thus implies that the behavior of b as a function of temperature changes character at each transition temperature. The well-known change at T_g is typical of that for a second-order transition. At T_{ll} there is a discontinuity in db/dT, characteristic of a third-order transition. We have discussed previously the tendency of T_{ll} to behave like a third-order transition (p 377, item 9, of ref 15).

B. Poly(*n*-butyl methacrylate) (PnBMA). The data of Olabisi and Simha[10] at $P = 1$, 100, 200, 300, and 400 bars were examined by means of eq 4. Figure 3 shows b^* vs. T at $T > T_g$. Two slope changes are noted: the first is at $T_{ll} = 95$ °C; the second, near 165 °C, corresponds to T_{ll}'. These same changes are evident in the point-to-point derivative plot, $-\Delta b/\Delta T$, especially for T_{ll}. There is no

Table II
Summary of Two-Line b^*–T Regression Analysis Parameters[a]

	polymer	set	temp range, °C	no. of data points	intercept, bars	slope, bars K⁻¹	R^2 [b]	std error,[c] bars	residuals pattern[d]
1.	PnBMA[10]	line 1	33.9–94.5	6	2159	−8.4439	0.99989	2.236	R
		line 2	94.5–160.2	6	1931	−6.0628	0.99817	7.230	NR
		quadratic[e]	94.5–160.2	6			0.99898	6.2258	NR
		quadratic[e]	105.6–160.2	5			0.99959	3.7620	R
		quadratic[e]	94.5–199.5	9			0.99936	6.0746	R
2.	PVAc[31]	line 1	45–70	5	1995	−6.9703	0.99864	2.856	R
		line 2	70–100	4	1934	−6.1060	0.99978	1.443	R
3.	iso-PMMA[9]	line 1[f]	59.1–90.4	4	2764	−9.4567	0.99951	3.456	NR
		line 2[f]	116.3–190.2	5	2457	−6.6226	0.99756	11.077	NR
4.	atactic PS[6]	line 1[f]	115.4–140.24	4	1907	−3.9146	0.99996	0.343	?
		line 2[f]	155.8–195.6	4	1835	−3.4236	0.99977	1.090	?
5.	atactic PMMA[10]	line 1[g]	113.5–159.0	5	2568	−6.8409	0.99945	4.161	NR
		quadratic 1	113.5–159.0	5			0.99992	1.535	R
6.	PCHMA[10]	line 1	122.7–158.2	4	2419	−7.2360	0.99614	8.52	?
		line 2	169.3–198.9	4	2151	−5.669	0.99441	6.59	?
7.	PoMS[6]	line 1	149.9–168.1	3	*h*	−7.9	*h*	*h*	*h*
		line 2	187.6–197.7	2	*h*	−4.9	*h*	*h*	*h*

[a] Quadratic and cubic models were applied to full data sets for each polymer but were rejected for several reasons given in the text. Parameters for ln b^*–T appear in Table IV. [b] Coefficient of correlation. [c] Standard error in calculated value of b^*. [d] Residuals, b^*(obsd) − b^*(calcd from the model), should be random about zero if the model selected was the correct one. When the number of data points is small, one cannot always decide between a random and nonrandom situation because of normal statistical fluctuations. Question marks are then used. [e] The nonrandom residuals pattern for line 2 suggested trying a quadratic above T_{ll}, which is a slightly better model. [f] Because of scatter in the b^*–T data and/or small number of data points for iso-PMMA and PS, A and γ parameters (see Table IV) were used to calculate values of b, which were then subjected to two-line regression analysis. [g] No isotherms were reported above 159.0 °C; T_{ll} from other sources is 165 °C; a quadratic through the five data points is marginally better than a straight line. [h] The paucity of data points did not justify regression analysis. b^* value for the 179.2 °C isotherm was high because of its proximity to T_{ll}. Slopes for b values calculated by Quach and Simha (averages for each isotherm) are −6.43 and −3.96 bars K⁻¹ for $\Delta(db/dT) = 2.47$ bars K⁻¹.

Table III
Summary of Parameters Relating to T_{II} from b^*-T[a]

polymer[b]	T_{II},[c] °C	density at T_{II},[d] g cm^{-3}	b^* at T_{II},[e] bars	$\Delta(db/dT)$ at T_{II},[f] bars K^{-1}	$\Delta\alpha$ at T_{II},[g] K^{-1}
1. PnBMA[10]	95	1.008	1360	2.238	0.89
2. PVAc[31]	70	1.153	1500	0.864	0.22
3. PVAc[11]	70		1470		0.22
4. iso-PMMA[9]	110	1.165	1725	2.834	1.29[h]
5. a-PS[6]	155	0.994	1300	0.491	0.21
6. a-PS[14]			1415		
7. a-PMMA[10]	165	1.120	1450	*i*	*i*
8. a-PCHMA[10]	165	1.039	1210	1.567	0.49
9. a-PoMS[6]	170-175	0.970	1220	3.0 2.47[j]	0.11

[a] b^* is the average value of b determined by eq 4 for $P \leq 400$ bars and is considered the correct value for b as $P \to 0$. All other parameters in this table are for $P = 1$ bar. [b] Arranged in order of increasing T_g. Numbers in parentheses are references to the original P-V-T data. [c] T_{II} from one or more of the sources listed in the Introduction as further confirmed from b^*-T plots. [d] Estimated from V_{sp}-T data in the references appearing in the first column. [e] Estimated from Figures 6 and 7. [f] Calculated from the slopes in Table II. [g] Calculated by us in a companion study[32] from V_{sp}-T plots at $P = 1$ bar, using data source in the references listed in the first column except where noted. [h] Calculated from data in Table 2 of ref 22 but cited in ref 32. $\Delta\alpha$ refers to a specimen of 60% isotactic and 40% syndiotactic content. [i] No P-V-T data available above T_{II}. Values of ρ and b^* at T_{II} extrapolated. [j] Lower value of Δb discussed in footnote *h* of Table II.

Table IV
Parameters for $b = A \exp(-\gamma T)$ at $P \leq 400$ bars and $T > T_g$

polymer	ref	A, bars	$-\gamma$, 10^{-3} K^{-1}	no. of data points	R^2[a]	std error in ln b	residuals pattern[b]	$-A\gamma$,[c] bars K^{-1}
1. PnBMA	10	2257	5.278	11	0.99948	0.00522	NR	11.912
		2272	5.363	14	0.99950	0.00668	NR	12.185
2. PVAc	31	2047	4.412	10	0.96915	0.01649	NR	9.031
3. PVAc (smoothed)	11	1887	3.453	6	0.99946	0.001924	R	6.516
4. iso-PMMA	9	2812	4.386	9	0.98261	0.0301	R	12.333
		2862	4.480	8	0.99057	0.0237	R	12.822
5. PS	6	2010	2.786	8	0.99005	0.00917	NR	5.600
6. PS	14	2206	4.119	10	0.78976[d]	0.1099[d]	NR	9.087
7. a-PMMA	10	2418	4.198	5	0.9996	0.00167	NR	10.150
8. PCHMA	10	2960	5.342	8	0.99877	0.0543	R	15.812
9. PoMS	6	2827	4.663	6	0.98845	0.0101	R	12.617

[a] Coefficient of correlation. [b] NR signifies nonrandom and R means random. [c] Slope of eq 3 is $db/dT = -A\gamma \exp(-\gamma T)$. [d] Very poor fit because ln b^*-T was not linear.

question about the two straight lines on either side of T_{II}. There are too few data points above 165 °C to characterize a third line with accuracy.

Figure 4 shows ln b^* as a function of T with a linear least-squares line through the data points. Parameters for this line appear in Table IV. Since R^2 for this line is 0.99950, the fit is near perfect. Indeed, visually, the fit is excellent. The top part of the figure plots the residuals against T. Here a residual is defined as ln b^*(obsd) − ln b^*(calcd), where ln b^*(calcd) is computed from eq 3 parameters. It is clear that these residuals, although small, are nonrandom about zero. The examination of residuals is one of several statistical techniques employed to analyze b^*-T results.[30]

Because of the comparatively large number of liquid-state isotherms available, PnBMA is an ideal candidate with which to illustrate and compare some alternate statistical procedures. We employ only the 11 liquid-state isotherms from 33.9 to 160.2 °C inclusive, which define the T_{II} region. We avoid the T_{II}' region because the three isotherms above it and the short temperature span of 25 K are insufficient to define a third linear section having statistical significance.

Figure 5 compares plots of $(Y - \hat{Y})/\mathrm{SE}(\hat{Y})$, where $Y - \hat{Y}$ is a residual as already defined and $\mathrm{SE}(\hat{Y})$ is the standard error in $\hat{Y}$. These quantities are usually available in computerized regression analysis programs. If the correct model has been selected to represent the data, $(Y - \hat{Y})/\mathrm{SE}(\hat{Y})$ values should lie randomly on either side of zero and fall within limits of ±2.[30]

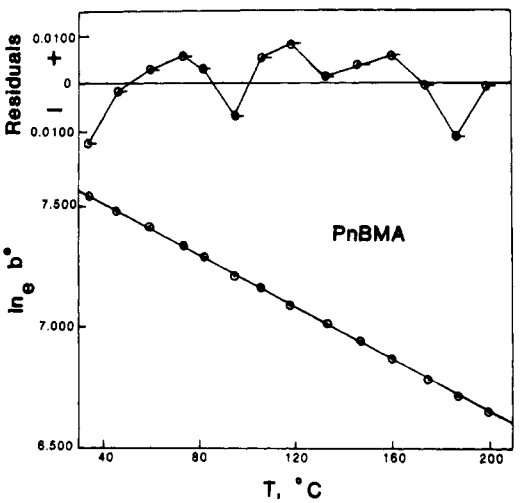

Figure 4. ln b^* vs. T for PnBMA using a linear least-squares regression line as shown, with b values from Figure 3. Top curve plots the nonrandom residuals pattern representing ln b^* − ln b(calcd), where the latter is a value of b computed from the least-squares line. A and γ parameters used are from Table IV.

Starting at the top of Figure 5 and progressing downward, the models employed are a cubic and a quadratic fit to b^*-T, the ln b^*-T model, and finally the two-line model intersecting at 94.5 °C. The top three models give

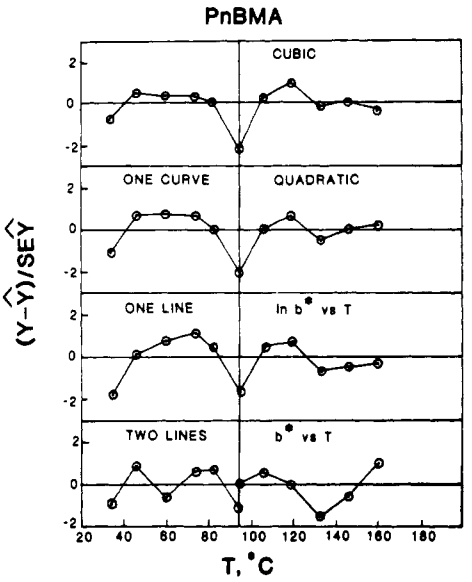

Figure 5. Plots of $(Y - \hat{Y})/\mathrm{SE}(\hat{Y})$ for cubic, quadratic, and two-line models of b^*–T and for the ln b^*–T model. The nonrandom patterns for the top three models rule them out mathematically. $Y - \hat{Y}$ is obtained from b^*(obsd) – b^*(calcd from the chosen model). $\mathrm{SE}(\hat{Y})$ is the standard error in b^*(calcd) and in ln b(calcd). Standard errors are 7.094 and 7.066 bars, respectively, for cubic and quadratic. Standard error for ln b–T is given in Table IV; that for two lines appears in Table II. $Y - \hat{Y}$ is same quantity as residuals in Figure 4.

distinctly nonrandom $(Y - \hat{Y})/\mathrm{SE}(\hat{Y})$ patterns, with a sharp minimum at T_{ll}. This is the $(Y - \hat{Y})/\mathrm{SE}(\hat{Y})$ pattern that must prevail if one tries to pass a monotonically curved function through two intersecting lines so as to minimize the standard error in $Y - \hat{Y}$: the residuals tend to alternate from – to + to – to + to – with increasing T, provided that the angle between the lines is not too small.

The two-line fit was prepared by breaking the punched card deck of b^*–T values into two sections, with the 94.5 °C values of b^* common to both. This is not arbitrary since it is suggested by inspection of Figure 3 and confirmed by the minima at 94.5 °C in Figure 4. The line from 33.9 to 94.5 °C gives a random pattern of $(Y - \hat{Y})/\mathrm{SE}(\hat{Y})$, a small standard error in b^*, and a high value of R^2. By these same criteria, a straight line from 94.5 to 160.2 °C is not as good. In fact, a mild quadratic through this upper set of points randomizes the residuals patterns, decreases the standard error, and increases R^2. See Table II for details.

The values of R^2 are generally quite high in all four models and hence are not too meaningful in differentiating between the various models. The ln b^*–T model gives an unusually small standard error in ln b^*, demonstrating how well ln b^* reproduces the data numerically. Only the $(Y - \hat{Y})/\mathrm{SE}(\hat{Y})$ pattern demonstrates that it is a mathematically incorrect model, as will be discussed in more detail in Appendix I.

The cubic, quadratic, and ln b^* models have also been applied to all 14 data points from 33.9 to 199.5 °C. The $(Y - \hat{Y})/\mathrm{SE}(\hat{Y})$ plots differ in details from those in Figure 4 but still have a large minimum at 94.5 °C in all three cases.

C. Isotactic PMMA (iso-PMMA). The data of Quach, Wilson, and Simha[9] were used. The b^*–T plot exhibited sufficient scatter that only data points above T_{ll} defined a good straight line. However, the eq 3 plot was quite linear, leading to a least-squares regression line with parameters listed in Table IV. From these, we calculated

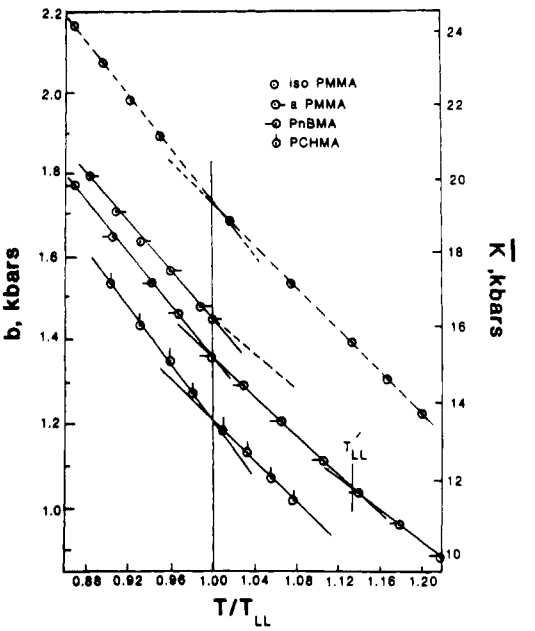

Figure 6. b vs. reduced temperature, T/T_{ll}, for the indicated polymers. Solid lines represent b^* calculated from eq 4 at $P \leq 400$ bars; dashed line is b calculated via eq 3, with A and γ values from Table IV. The right-hand ordinate is bulk modulus, $\bar{K}$, for $P \rightarrow 0$, calculated from $\bar{K} = b/C'$. Lines shown are not linear least-squares lines.

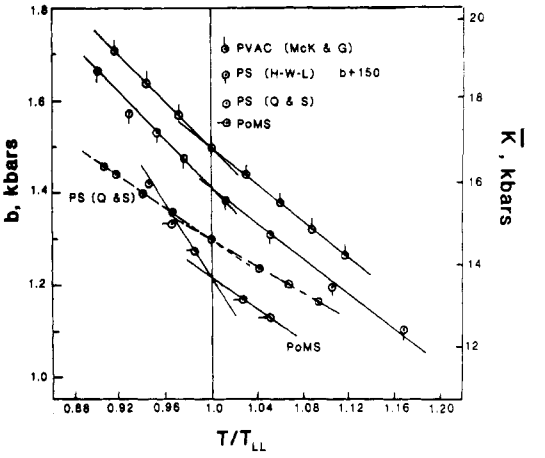

Figure 7. b vs. reduced temperature, T/T_{ll}, for the indicated polymers. PoMS represented b^* values. Others are b calculated via eq 3 method.

values of b at each temperature for which isothermal data existed. The results are shown in Figure 6.

D. Atactic Polystyrene. The P–V–T data of Hellwege et al.[14] were used by Simha et al.[7] to calculate the b–T results shown in Figure 1. The low T_g of this specimen, $T_g \sim 88$–89 °C at $P = 1$ bar, implies that it contained oligomeric material—monomer, dimers, and trimers characteristic of commercial thermal PS's at that time. Hence these data will not be subjected to further study. The thermal PS specimen of Quach and Simha,[6] with a T_g of 101 °C, is more typical of pure PS. However, only three isotherms covering a temperature range of 22 K above T_{ll} cannot yield a well-defined line. Hence we have used a ln b^*–T plot to obtain the A,γ values given in Table IV, from which a b^*–T plot was prepared. These results are shown in Figure 7.

E. Poly(*o*-methylstyrene) (PoMS). P–V–T data on this polymer were determined at seven liquid-state isotherms from 139.4 to 197.7 °C.[7] V–T and ρ–T plots at P

= 1 bar suggested a slope change at about 175 °C indicative of T_{ll} and this is confirmed by a slope change in the b^*–T plots. ρ is density in g cm^{-3}.

F. Poly(vinyl acetate) (PVAc). The V_{sp} data of McKinney and Goldstein[31] were given to five significant figures at 5 K intervals, apparently as the result of a smoothing operation. The plot of b^* from eq 4 against T showed unexpected scatter but still defined two straight lines. Recourse was taken again to the ln b^*–T method, which did not eliminate the scatter but appeared to define an acceptable line whose parameters appear in Table IV. Values of b^* calculated therefrom are plotted in Figure 7.

Beret and Prausnitz[11] gave values of $1 \simeq V/V_0$ for PVAc in the temperature range 64–120 °C, compared to 40–100 °C (liquid state) by McKinney and Goldstein. Values of b^* vs. T from their smoothed data clearly fell low on a different line from those of McKinney and Goldstein. A straight line below T_{ll} could not be defined for lack of isotherms below 64 °C. However, the exponential procedure permitted us to calculate values of b below T_{ll} using parameters listed in Table IV. Only the data of McKinney and Goldstein are used in Figure 7.

G. Atactic PMMA. T_{ll} has been determined for this polymer by a variety of methods (see Table 3 of ref 22). T_{ll} is dependent on tacticity[33] but for a PMMA of about 70% syndiotactic content, it falls near 165 °C. We are not aware of any P–V–T data in the literature above T_{ll}. Olabisi and Simha[10] did report P–V–T data in the liquid state from 113.5 to 159.0 °C with five isotherms. b^* was determined in this range for use in some later correlations. The b^*–T plot was nearly linear as may be judged from information presented in Tables II and III but gave nonrandom residuals suggestive of a mild quadratic.

Discussion of Results

Table II collects the various statistical parameters resulting from the two-line b^*–T regression analysis studies. These same b^*–T data were also analyzed by quadratic and cubic models as discussed for PnBMA in connection with Figure 5.

Several factors may favor apparent superiority of polynominals over a two straight line model: (1) small number of data points, (2) scatter in data, and (3) smaller slope change in b^*–T across T_{ll}. R^2 tends to be higher since the polynomial uses all data points; each straight line uses about half the data points. Even so, the two-line model was generally slightly better than, or about the same as, the quadratic model in standard error. The cubic was not appreciably different from the quadratic as seen in Figure 5. Moreover, the polynomial fits required alternation in signs of the coefficients of the terms in the equation: +, −, + for the quadratic; +, −, +, − for the cubic. This alternation in sign permits a polynomial of degree n to approach the two intersecting straight line model as a limit with increasing n. Even more significant than any of the above evidence is the fact that the largest negative residual in the quadratic and cubic models for all polymers occurs at or near T_{ll}, as was demonstrated so well for PnBMA in Figure 5.

We therefore conclude that the two straight line model is the correct way to represent the b^*–T data for all polymers. It is not only statistically superior but also conveys a physical meaning to b vs. T which is lacking in the exponential model. Some improvement in matching data may be possible, using a more sophisticated model. The combination of a straight line and a quadratic as with PnBMA is such a case. The availability of more accurate P–V–T and especially of closer temperature and pressure intervals may dictate the use of two quadratics on either side of T_{ll}.

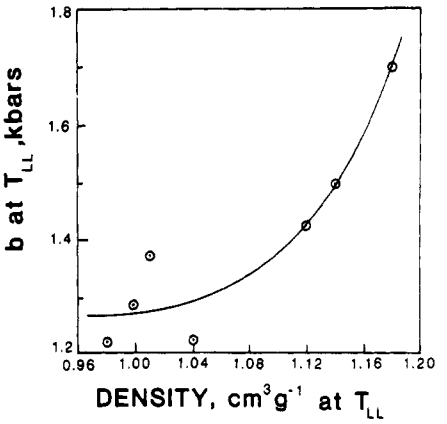

Figure 8. b at $T/T_{ll} = 1$, as read from Figures 6 and 7, plotted against polymer density, ρ (g cm^{-3}) at T_{ll}. A plot of b^* against ρ^3 is approximately linear.

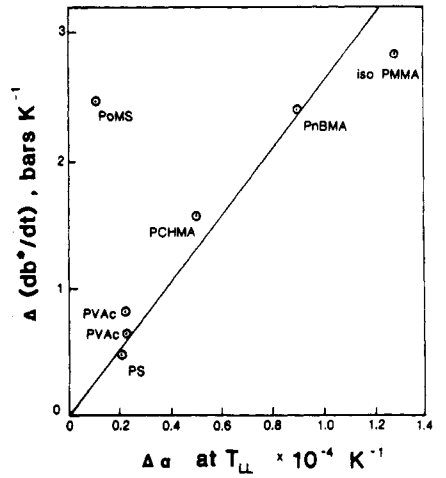

Figure 9. Difference in slopes across T_{ll}, $\Delta(db^*/dT)$, from Table III plotted against differences in coefficient of thermal expansion across T_{ll} from ref 32 as listed in Table III. Deviation of PoMS is not understood.

We wish now to offer further evidence for the validity of the two-line model by means of various correlations using quantities assembled in Table III. In order to compare b^*–T plots for the several polymers, we employ a reduced temperature scale. Figure 6 compares the four polymethacrylate esters. The horizontal shift shows general similarity in the four plots.

Figure 7 is a similar plot for PoMS, the two sets of PS data, and one set of PVAc data. The striking differences between the two sets of PS, in both slopes and general level after correction for the plotting displacement, are evident.

Considering T_{ll} as a reference state, we have made a correlation between b^* at T_{ll} and polymer density ρ at T_{ll} as seen in Figure 8. While this correlation was empirical in origin, it is logical that bulk modulus should depend in some way on density. PnBMA and PCHMA are reversed in position on Figure 8, for which we have no explanation. Several other correlations with density were attempted. Plots of b^* against ρ consisted of two straight lines of positive slope intersecting at T_{ll} for PCHMA and iso-PMMA and three lines intersecting at T_{ll} and T_{ll}' for PnBMA. A plot of db^*/dT against $d\rho/dT$ for $T_g < T < T_{ll}$ was roughly linear through 0,0 for the four methacrylates and PoMS but for PS and PVAc it fell well below the trend line.

We indicated in the Introduction that the slope change

across T_{ll}, $\Delta(db/dT)$, was a possible measure of the strength of T_{ll}. Figure 9 is a correlation of $\Delta(db/dT)$ at T_{ll} with $\Delta\alpha$ at T_{ll}. The most serious problem is the point for iso-PMMA, where $\Delta(db/dT)$ is pure iso-PMMA, while $\Delta\alpha$ is for 60% iso-PMMA. Since $\Delta\alpha$ at T_g has been considered to be a measure of the strength of T_g, we have assumed elsewhere that $\Delta\alpha$ at T_{ll} is a measure of the strength of T_{ll}.[32] Incidentally, $\Delta\alpha$ at T_{ll} is in the range 5–40% of $\Delta\alpha$ at T_g, being smallest for PS and PVAc. It does appear that the slope change $\Delta(db^*/dT)$ across T_{ll} is also some indication of the strength of T_{ll}. We conclude that T_{ll} tends to be stronger in the methacrylates than in PVAc or PS. Based on $\Delta(db/dT)$, T_{ll} is stronger in PoMS than in PS. Chain stiffness and/or polarity contribute to the strength of T_{ll} (see discussion on phase dualism on pp 540–42 of ref 22).

Finally, to complete the results, Table IV lists the eq 3 parameters A and γ for the ln b^*–T linear regression analysis. Comparison with the literature values of A and γ from Table I shows marked similarity for PnBMA, PVAc(McK–G), and PCHMA, marked dissimilarity for PVAC(B–P) and PS(H–K–L), and reasonable agreement for iso-PMMA and PS(Q–S). Values which differ appreciably are readily explained by the several procedures employed. For example, Beret and Prausnitz used the entire isotherms and a higher value of C. Values that are quite similar imply that the literature method calculated b at low pressures only, that b does not increase much at a pressure-induced transition, or that eq 1 is obeyed across the entire isotherm.

The slope of eq 3 is

$$db/dT = -A\gamma \exp(-\gamma T) \tag{5}$$

The quantity $-A\gamma$ is listed in Table IV. Values of the slopes at T_{ll} = −30 K and T_{ll} = +30 K were calculated but are not shown. The difference in slopes from T_{ll} = −30 K to T_{ll} = +30 K are generally slightly different from $\Delta(db/dT)$ values of Table III for the two-line method.

Summary and Conclusions

1. The Tait equation parameter, b, calculated from isothermal volume–pressure data by a linear form of the Tait equation (see eq 4) at low pressures ($P \leq 400$ bars) gives plots against temperature consisting of two straight lines intersecting at the liquid–liquid transition temperature, T_{ll}, as determined by other methods. Values of b thus calculated are designated b^* to distinguish them from values of b obtained by other methods and/or by the same method at higher pressures. b^* values tend to be smaller than b values reported in the literature as averages for an entire isotherm (see Figure 1) or b values calculated by eq 4 at high pressures. This is because of pressure-induced transitions.

2. The physical interpretation of this two-line behavior is that the bulk modulus, $\bar{K}$ ($=b/C'$ at $P \rightarrow 0$), in bars, has a different temperature coefficient, $d\bar{K}/dT$, above and below the T_{ll} transition, being smaller above than below T_{ll}. Alternately, the isothermal compressibility, κ ($=C'/b$), has a larger temperature coefficient above T_{ll} than below.

3. b^* at T_{ll} increases nonlinearly with polymer density, ρ, at T_{ll}, where ρ is estimated for P = 1 bar.

4. The slope difference in b across T_{ll}, $(db/dT)_l - (db/dT)_{ll}$, in units of bars K^{-1}, is proportional to the difference in coefficients of cubical expansion across T_{ll}, i.e., $\alpha_l - \alpha_g$, in units of K^{-1}. T_{ll} is stronger in the polymethacrylate esters than in PVAC or the polystyrenes.

5. The two-line b^*–T representation is, in most cases, numerically, if not mathematically, equivalent to the exponential representation $b = A \exp(-\gamma T)$ found in the literature, as summarized in Table I. b^*–T parameters A and γ have been calculated and are listed in Table IV.

6. The two-line and exponential b^*–T numerical equivalence arises because (a) the range in b values for any polymer is within a factor of about 2 and (b) values of b^* calculated from either method are at relatively large temperature intervals of 15–20 K. Also, random errors in the experimental b^* values may mask any possible curvature in the ln b–T plots.

7. While the two-line b–T representation is considered scientifically correct, the exponential form has two advantages which justify its continued use: (a) It permits smoothing by linear regression when scatter in the data is greater than average and/or when the number of liquid-state isotherms below and/or above T_{ll} is too few. (b) It permits volumetric data to be calculated as a function of both pressure and temperature in a simple extension of the Tait equation as in ref 11.

8. There is a discontinuity in b (and $\bar{K}$) at T_g (Figure 2) characteristic of a second-order transition, but a discontinuity in db/dT (and $d\bar{K}/dT$) at T_{ll} characteristic of a third-order transition. (See Table III).

9. The intersection temperature for the two-line b^*–T plots thus provides thermodynamic-type evidence for the existence of the liquid–liquid transition.

10. Comparison of b^*–T plots for a series of polymers is conveniently achieved by plotting b^* against a reduced temperature T (K)/T_{ll} (K).

11. In one instance, PnBMA, a b^*–T plot above T_{ll} consists of two lines intersecting at the T_{ll}' transition.

12. All conclusions about b^*–T in this paper are based on regression analysis using one, two, or three lines as well as quadratic and cubic models for b^*–T and a one-line model for ln b^*–T. (See parameters in Tables II and IV.)

Acknowledgment. I am indebted to Dr. K. Šolc for eq 4 and to Ms. Kathleen Panichella for the regression analysis studies and for the artwork. The manuscript was prepared by Ms. Joan Summers.

Appendix I. Two-Line vs. Exponential Representation of b–T

The various studies just discussed repeatedly verified the numerical, if not mathematical, equivalence in representing b–T values either by two straight lines or as the exponential eq 3 relationship. As a final check, we prepared a graphical construction of two intersecting lines defined by the three coordinates T = 110 °C, b = 1600 bars; T = 165 °C, b = 1200 bars, the intersection point; and T = 1230 °C, b = 900 bars. The slopes of the lines were −7.212 and −4.706 bars K^{-1}, similar to values in Table III. Values of b were estimated from this plot at 20 K intervals, thus ensuring some random errors in b. A least-squares regression line followed the equation

$$b = 2736 \exp(-4.888 \times 10^{-3} T) \tag{6}$$

whose parameters are similar to those in Tables I and IV. The fit was characterized by R^2 = 0.999568. A residuals plot (not shown) between values read from the two lines and those calculated from eq 6 was distinctly nonrandom, with the largest residual being negative and occurring at the intersection.

This exercise with synthetic data and the various studies with real b–T data have caused us to pose two questions: (1) Why is there such numerical identity between two intersecting straight lines and an exponential representation? (2) Which representation is to be preferred? Our

answer to the first question is as follows:

1. The range in b values for any single polymer is small and at most a factor of 2. The range for all polymers is from about 800 to about 2000 bars.

2. Calculation of b values using A and γ parameters is usually made at intervals of 10–20 K, corresponding to the relatively large intervals between the original isotherms, so that the curvature which must be present is not readily noticed.

3. Random errors in experimental b values also tend to obscure curvature in the ln b–T plots.

4. The angle between each pair of straight lines is small, at most a few degrees.

We propose two answers to the second question. First, assuming the T_{II} transition to be real (and this has been contested as discussed in ref 19), it is physically more satisfying if a fundamental material property such as the bulk modulus, $\bar{K}$, and consequently b, exhibits a change in behavior with temperature across that transition. As a consequence of the present study, we now reverse this proposition and state that since b vs. T does change slope at a specific temperature, this validates the existence of the transition in question. It further provides a thermodynamic type of evidence for T_{II} to substantiate other types of physical evidence for T_{II} cited in the Introduction as ref 15–27.

A second and coexisting answer to question 2 is that eq 3, with only two parameters, is far more convenient for engineering and other calculations than are two straight lines which imply five parameters, namely, two intercepts, two slopes, and an intersection. Thus, Beret and Prausnitz[11] have substituted eq 3 into eq 1 to yield a convenient expression which represents volume as a function of both T and P. We have used eq 3 plots on several occasions when scatter in the b–T data and/or an insufficient number of data points caused problems in defining two straight lines.

Therefore, we suggest use of the two-line representation for rigor and physical meaning but the exponential one for convenience when the occasion demands.

References and Notes

(1) Wood, L. A.; Martin, G. M. *J. Res. Natl. Bur. Stand., Sect. A* **1964**, *68A*, 259.
(2) Wood, L. A. *J. Polym. Sci., Polym. Lett. Ed.* **1964**, *2*, 703.
(3) Nanda, V. S.; Simha, R. *J. Chem. Phys.* **1964**, *41*, 3870.
(4) Gee, G. *Polymer* **1966**, *7*, 177.
(5) Quach, A.; Simha, R. *Macromolecules* **1971**, *4*, 268.
(6) Quach, A.; Simha, R. *J. Appl. Phys.* **1971**, *42*, 4592.
(7) Simha, R.; Wilson, P. S.; Olabisi, O. *Kolloid Z. Z. Polym.* **1973**, *251*, 402.
(8) McKinney, J. E.; Simha, R. *Macromolecules* **1974**, *7*, 894. See also ref 31.
(9) Quach, A.; Wilson, P. S.; Simha, R. *J. Macromol. Sci., Phys.* **1974**, *B9*, 533.
(10) Olabisi, O.; Simha, R. *Macromolecules* **1975**, *8*, 206.
(11) Beret, S.; Prausnitz, J. J. *Macromolecules* **1975**, *8*, 536.
(12) Lichtenthaler, R. N.; Liu, D. D.; Prausnitz, J. M. *Macromolecules* **1978**, *11*, 192.
(13) Kubota, K.; Ogino, K. *Macromolecules* **1978**, *11*, 514.
(14) Hellwege, K.-H.; Knappe, W.; Lehmann, P. *Kolloid Z. Z. Polym.* **1963**, *183*, 110.
(15) Boyer, R. F. *Macromolecules* **1981**, *14*, 376.
(16) Boyer, R. F. *Colloid Polym. Sci.* **1980**, *258*, 760.
(17) Gillham, J. K.; Boyer, R. F. *J. Macromol. Sci., Phys.* **1977**, *B13*, 497.
(18) Cowie, J. M. G. *Polym. Eng. Sci.* **1979**, *19*, 709.
(19) Boyer, R. F. *Polym. Eng. Sci.* **1979**, *19*, 732.
(20) Gillham, J. K. *Polym. Eng. Sci.* **1979**, *19*, 749.
(21) Enns, J. B.; Boyer, R. F.; Ishida, H.; Koenig, J. L. *Polym. Eng. Sci.* **1979**, *19*, 756.
(22) Boyer, R. F. *J. Macromol. Sci., Phys.* **1980**, *B18*, 461–553.
(23) Boyer, R. F.; Heeschen, J. P.; Gillham, J. K. *J. Polym. Sci., Polym. Phys. Ed.* **1981**, *19*, 1321.
(24) Smith, P. M.; Boyer, R. F.; Kumler, P. J. *Macromolecules* **1979**, *12*, 61. See also: Smith, P. M. *Eur. Polym. J.* **1979**, *15*, 147.
(25) Boyer, R. F. *Eur. Polym. J.* **1981**, *17*, 661.
(26) Keinath, S. E.; Boyer, R. F. *J. Appl. Polym. Sci.* **1981**, *26*, 2077.
(27) Lacabanne, C.; Goyaud, P.; Boyer, R. F. *J. Polym. Sci., Polym. Phys. Ed.* **1980**, *18*, 277.
(28) Šolc, K. Michigan Molecular Institute, private communication, Aug 1980. We have subsequently learned from other private communications that eq 4 is in general use for regression analysis of V–P data, calculation of b, etc.
(29) Šolc, K.; Keinath, S. E.; Boyer, R. F., manuscript in preparation.
(30) For a general discussion on the use of residuals in regression analysis, consult Gunst and Mason (Gunst, R. F.; Mason, R. L. "Regression Analysis and Its Applications"; Marcel Dekker: New York, 1980) or standard textbooks on regression analysis. For a detailed discussion of the specific residuals techniques used herein see: Boyer, R. F.; Miller, R. L.; Parks, C. N. J. *Appl. Polym. Sci.* **1982**, *27*, 1565.
(31) McKinney, J. E.; Goldstein, M. *J. Res. Natl. Bur. Stand., Sect. A* **1974**, *75A*, 331. Tabular data in this paper were analyzed by eq 1 in ref 8.
(32) Boyer, R. *Macromolecules*, in press.
(33) Denny, L. R.; Boyer, R. F.; Elias, H.-G.; Gillham, J. K. *Org. Coat. Plast. Chem.* **1980**, *42*, 682.